An Experimental Study on the Effect of Methane Potent Biogas Mixture on Gas Permeation Mechanism

Priscilla Ogunlude*, Idris Hashim*, Muktar Ramalan* Evans Ogoun*, Firdaus Muhammad-Sukki**, Ayo Giwa***, and Edward Gobina*

* Centre for Process and Membrane Technology, Robert Gordon University, Aberdeen, United Kingdom, e.gobina@rgu.ac.uk
**School of Engineering & the Built Environment, Edinburgh Napier University, United Kingdom, F.MuhammadSukki@napier.ac.uk
***McAlpha Inc, Calgary, Canada, info@mcalpha.com

ABSTRACT

This study focuses on the use of composite alumina membranes for the separation of carbon dioxide from methane. The technique can be applied to pre, post and oxy-combustion operations in industry and would be particularly useful in mitigating the effect of greenhouse gases in our world today. The porous tubular ceramic supports used in this study were tailor made by Ceramiques Techniques et Industrielles (CTI SA) in France consisting of an alumina support and separation layer of pore sizes ranging from 15 – 6000nm. The membrane layers are fixed on the support, starting with very coarse (intermediate) layers then more layers with decreasing pore sizes are added until the designated pore sizes are reached. For example, to achieve a membrane with the pore size of 6000nm, the support will have one layer (1) of a macroporous membrane, while a membrane with pore size of 200nm will have the support plus layer (1) and layer (2). Again, to achieve a membrane with mesoporous size of 15 nm, we will have the support plus layers (1 + 2 + 3). The layers are made from different materials such as aluminium oxide (Al_2O_3), titanium oxide (TiO_2), zirconium oxide (ZrO_2), silicon dioxide (SiO_2), silicon carbide (SiC). Materials are carefully selected so that they are thermally compatible with the support to prevent delamination or crack formation at elevated temperatures.

Keywords: emissions, climate change, permeation, biogas, net-zero, membranes

1 BACKGROUND

The Net-Zero Emissions by 2050 Scenario does require that all non-emergency flaring be eliminated globally by 2030, implying roughly a 90% reduction in flared volumes by 2030. New projects must incorporate strategies to utilize associated gas or to safely reinject it underground. For existing fields, an optimal solution would involve directing associated gas to a localised gas market. From October 31 to November 12, 2021, the 26th UN Climate Conference (COP26) was held in Glasgow in which 197 countries took part to define a road map aimed at achieving the goal of containing global warming by 1.5°C and reaching climate neutrality (zero emissions). The EU Commission Chief Ursula von der Leyen and the US President Joe Biden announced a global pledge to cut methane emissions 30% by 2030.

Methane pollution from fossil fuels, agriculture, and waste account for over one-quarter of today's warming. Heightened awareness over the need for climate actions that target the pollutants affecting both the scale and the speed at which the planet is warming has brought acute focus on methane. In the absence of the local markets, however, or where fields are very remote, several technologies can offer the productive use of the associated gas while working towards the longer-term reduction objective in fossil fuel use modelled in the Net Zero Emissions by 2050 Scenario.

Despite global oil demand dropping nearly 7% in 2020 (precipitated by the Covid-19 pandemic), flaring fell by only 5%. Globally, 142 billion m^3 of natural gas was flared in 2020 which is roughly equivalent to the natural gas demand of Central and South America. This resulted in around 265 Mt CO_2, nearly 8 Mt of methane (240 Mt CO_2-eq) and black soot and other greenhouse gases (GHGs) being directly emitted into the atmosphere. The emission of GHGs has been confirmed to be a major factor affecting global warming with the most potent being methane and carbon dioxide [1-5]. When these gases are released into the atmosphere and accumulate in sufficient quantities, they cause heat to be trapped (i.e. do not allow heat to dissipate into space) and this causes an imbalance in the amount of energy that comes from the sun to the earth and back. This leads to changes on the earth surface temperature and causes temperature increments resulting in warming that create droughts and other alterations in the ecosystem.

A suitable means of capturing GHG emissions has now become a matter of global urgency and membrane technology has been identified as a suitable technique to meet the net-zero emissions target. A membrane may be defined as a permeable or semi-permeable layer which controls the flow of compounds and hence delivers one product with less of another component thus resulting in the product concentration in those component [6]. This process

is used in industry for recovery of reactants and valuable gases, isolation of products and pollution control [7]. The flow of gases is based on their differences in permeability which is a function of membrane properties and the nature of gases [8]. Generally, the performance of a membrane is defined by its permeability and selectivity and a good indication is with high values of both achieved for efficiency in commercial applications but in practicality, there is a trade-off between these parameters. However, in any given process, there is an economic optimum in the combination of selectivity and permeance.

The porous tubular ceramic membranes used throughout the research were tailor made by Ceramiques Techniques et Industrielles (CTI SA) in France consisting of an alumina support and separation layer of pore sizes ranging from 15 – 6000nm. The membrane layers are fixed on the support, starting with very coarse (intermediate) layers; membrane layers with decreasing pore sizes are added until the designated pore sizes are reached as shown in Fig. 1.

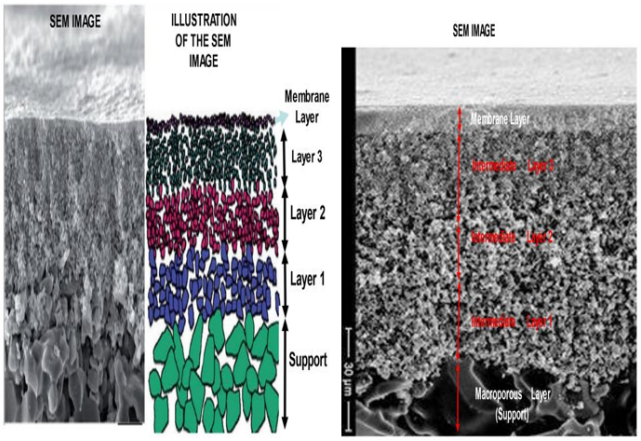

Figure 1: Scanning electron microscopy and illustration of the layered arrangement of a typical ceramic membrane structure.

For example, to achieve a membrane with the pore size of 6000nm, the support will have layer (1) to achieve a macroporous membrane, while a membrane with pore size of 200nm also macroporous will have the support plus layer (1) and layer (2). Again, to achieve a membrane with mesoporous size of 15nm, we will have the support plus layers (1 + 2 + 3). Subsequent pore size reductions to get to the microporous size will added to the top layer on this structure to get down to < 2nm. The layers are usually made from different materials such as aluminium oxide (Al_2O_3), titanium oxide (TiO_2), zirconium oxide (ZrO_2), silicon dioxide (SiO_2), silicon carbide (SiC), Zeolite or a hybrid mixture of two or more materials of their oxides can be used for the fabrication of different layers of the composite ceramic membranes and are carefully selected so that they are thermally compatible with the support to prevent delamination or crack formation at elevated temperatures.

Furthermore, silica membranes have been fabricated by dip coating the alumina membranes. Dip coating was done to enhance the performance of these membranes in terms of selectivity by modifying the membrane properties.

Silicone membranes are some of the best performing ceramic membranes for gas separation and have been studied based on many fluid forms to achieve high permeability and selectivity. However, there has only been little research into elastomeric materials for gas separation, even though, rubbery polymers reveal very high gas fluxes compared with glassy polymers that are also limited by poor adhesion.

2 METHODOLOGY

The membranes used in this study consists of an alumina support with mean pore diameters of 15, 200 and 6000nm respectively with a TiO_2 wash coat top layer. Nitrogen adsorption-desorption measurements are carried out using Automated Gas Sorption Analyser by Quantachrome Instruments at 77K to determine the Brunaer - Emmett - Teller (BET) surface area of the support membranes, and to estimate the pore size distribution and pore volume respectively. Samples were also examined with a scanning electron microscope (SEM) energy dispersive Analysis X-rays (EDXA).

Gas permeation and stability tests were conducted to observe the gas behaviour and mechanism under varied operating conditions of temperature and pressure. The permeation system used in this study consists essentially of the gas delivery system, permeation cell and flow measurement. The gases were admitted into the shell-side and allowed to permeate through the support membrane at a predetermined pressure differential as shown in Fig 2.

Figure 2: Experimental Permeation Rig.

3 RESULTS AND DISCUSSION

3.1 Scanning Electron Microscope (SEM) Energy Dispersive Analysis X-Rays (EDXA)

SEM imaging was carried out to study the microstructure, surface and cross-sectional morphology of the membrane. This analysis was carried out using a Zeiss Evo LS10 S with an Oxford Instruments INCA System Energy Dispersive X-ray Analyser. Samples were prepared by carefully cutting a fragment of the membrane. A clean pair of tweezers were used to pick the sample to mount on the stub for analysis and the results are shown in Fig. 3.

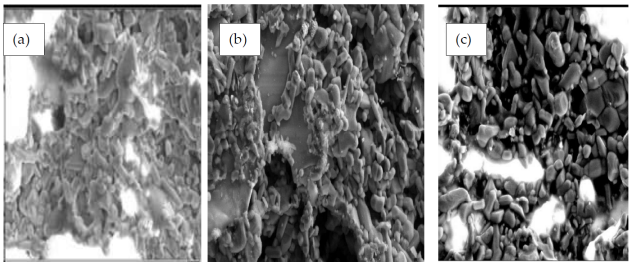

Figure 3: SEM Micrographs of membranes with pore sizes (a) 15nm (b) 200nm (c) 6000nm.

3.2 Gas Permeation

Permeability was measured by the classical steady-state flow method in which a differential pore pressure, ΔP or tans-membrane pressure drop is maintained and the flow rate flowing out from the downstream or permeate side of the samples is monitored using an electronic flowmeter. The pressure drop was controlled by the gas regulator for gas permeability measurement and the downstream pressure was released to atmospheric pressure, assumed constant of 0.1MPa. The two most important performance indicators for a gas separation membrane are the permeance and ideal selectivity (or perm-selectivity). The gas flux, Q, can be estimated using the following expression (Equation (1)):

$$Q = \frac{q}{A} = -\kappa \frac{\Delta P}{\mu \delta} \tag{1}$$

where:

q	molar flowrate, $mols^{-1}$
A	cross-sectional area of the porous medium perpendicular to the flow, m^2
Q	fluid Volume flux, $molm^{-2}s^{-1}$
κ	absolute permeability, m^2
ΔP	pressure difference (Pa) across the distance L parallel to the direction of flow, m
μ	the fluid viscosity, Pa-s
δ	finite distance, m

The permeance F_T is defined as the ratio of the permeability coefficient (K) to the membrane thickness (δ) as presented in Equation (2). The permeance for a given constituent diffusing through a membrane with a defined thickness is analogous to a mass transfer coefficient

$$F_T = \frac{\kappa}{\delta} \tag{2}$$

where,

κ	absolute permeability, m^2
δ	finite distance, m

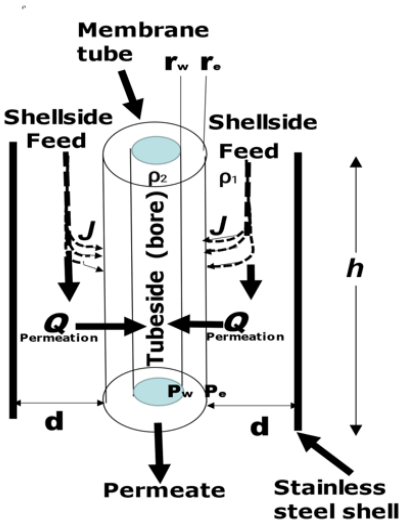

Figure 4: Description of external mass transfer rates are changing with the gas stream velocity.

The membranes used for analysis are tubular form as in Fig. 4 and thus Equation (1) is altered and the gas volume flux can be estimated by using Equation (3):

$$Q_i = \frac{\kappa_i \left(\frac{dp_i}{dx}\right)}{\mu_i} \tag{3}$$

The mass transfer flux can then be calculated using the following Equation (4):

$$J_i = (\rho_1 - \rho_2) \frac{ShDe_i}{d} \tag{4}$$

where,

ρ_1, ρ_2	respective molar gas densities on the shell and permeate sides respectively, $gmolcm^{-3}$
De	diffusivity of gas in the shell-side, cm^2s^{-1}
d	annular diameter, cm
Sh	Sherwood number

Table 1 shows the results from the experimental study. The performance of classical dense membranes compared to these porous systems is limited by the low permeability although it possesses high selectivity. In all situations of temperature and pressure drops investigated on the porous membrane, mass transfer rate from the bulk gas stream to the membrane surface was significantly greater than the permeation rate, this confirms that mass transfer conditions are not limiting. Table 1 reveals that, under the same pressure drop across the membrane, the mass/volume flux in porous membrane can be over four orders of magnitude higher than in a PDMS membrane with the similar thickness due to the different gas transport mechanisms at play.

Table 1: Mass transfer characteristics of gas flow through each membrane.

Pore Size (nm)	Permeability ($x10^{-13}$ m^2)	Gas mass transfer flux from the bulk gas in the shell-side to the membrane outer surface, J_{CH4} ($x10^{-3}$ g/cm^2s)	Gas mass transfer flux from the bulk gas in the shell-side to the membrane outer surface, J_{CO2} ($x10^{-3}$ g/cm^2s)
15	1.8	5.82 – 71.6	10.5 – 129.3
200	1.5	6.13 – 75.4	11.1– 136.2
6000	0.49	1.87 – 23.0	3.39 – 41.6

4 CONCLUSION

This paper uses data derived from experimental studies to determine the factors that increase perm-selectivity of the membranes having different physical properties. It was found that:

- The performance of classical dense membranes compared to these porous systems is limited by the low permeability although it possesses high selectivity.
- In all situations of temperature and pressure drops investigated on the porous membrane, mass transfer rate from the bulk gas stream to the membrane surface was significantly greater than the permeation rate, this confirms that mass transfer conditions are not limiting.
- The mass flux of each component is determined based on the partial pressure of the gases and membrane properties
- For a thicker membrane, having more flow resistance within the layer, the mass flux of the gases is reduced.

5 REFERENCES

[1] Lashof DA, Ahuja DR. Relative contributions of greenhouse gas emissions to global warming. Nature. 1990;344(6266):529.

[2] Yang N-T, Kathiraser Y, Kawi S. La0. 6Sr0. 4Co0. 8Ni0. 2O3− δ hollow fiber membrane reactor: Integrated oxygen separation–CO2 reforming of methane reaction for hydrogen production. International journal of hydrogen energy. 2013;38(11):4483–91.

[3] Kim J, Maiti A, Lin L-C, Stolaroff JK, Smit B, Aines RD. New materials for methane capture from dilute and medium-concentration sources. Nature communications. 2013;4(1):1

[4] Shindell D, Kuylenstierna JC, Vignati E, van Dingenen R, Amann M, Klimont Z, et al. Simultaneously mitigating near-term climate change and improving human health and food security. science. 2012;335(6065):183–9.

[5] Kuylenstierna J, Zucca M, Amann M, Cardenas B, Chambers B, Klimont Z, et al. Near-term climate protection and clean air benefits: Actions for Controlling Short-Lived Climate Forcers. 2011;

[6] Ozen HA, Ozturk B. Gas separation characteristic of mixed matrix membrane prepared by MOF-5 including different metals. Separation and Purification Technology. 2019;211:514–21.

[7] Beil M, Beyrich W. Biogas upgrading to biomethane. In: The Biogas Handbook [Internet]. Elsevier; 2013 [cited 2019 May 6]. p. 342–77. Available from: https://linkinghub.elsevier.com/retrieve/pii/B9780857094988500154

[8] Sridhar S, Bee S, Bhargava S. Membrane-based gas separation: principle, applications and future potential. Materials Science. 2014;